Indian Journal of Chemical Technology
Vol. 30, November 2023, pp. 765-779
DOI: 10.56042/ijct.v30i6.3654

Effect of CuO nano additive with novel punnai methyl ester in a TBC CI engine

A Vadivel[1]* & R Vinoth[2]

[1]Department of Mechanical Engineering, Sri Ramakrishna Engineering College, Coimbatore, Tamil Nadu, 641 022, India

[2]Department of Mechanical Engineering, Excel Engineering College, Namakkal, Tamil Nadu, 637 303, India

*E-mail: mech_vadivel@yahoo.co.in

Received 10 July 2023; accepted 2 October 2023

The requirement for petroleum fuel has amplified due to the growth of automobile industries and population growth. To meet fossil fuel demand in the future, alternative fuel for diesel fuel is necessary. The technique for engine modification is also considered as the latest advance in engine research aimed to complete combustion. The engine has been coated with a mixture of a ceramic thermal barrier material of 88% Yttria Stabilized Zirconia (YSZ), 4% Magnesium oxide (MgO), and 8% Titanium oxide (TiO_2) of 150 µm thickness by the plasma spray process. After engine modification, the coated engine has been analyzed with the mixing of Copper oxide (CuO) nanoadditive to the B20 Punnai Methyl Ester. The structural and chemical constituents of the biofuel are determined using Fourier transform infrared spectroscopy and gas chromatography. The test result noted that brake thermal efficiency is increased by 17.14% for the coated engine as compared to the uncoated engine. The brake specific fuel consumption for the tested fuel used in the coated engine is decreased by 11.16%. Engine emission parameters are reduced especially oxides of nitrogen (NO_x) emission of 10.84% for the tested fuel in the coated engine.

Keywords: Biodiesel engine, Copper oxide nanoadditive, Engine emission parameter Punnai methyl ester, Thermal barrier coating

Energy demand is currently far away and will not be managed in the future due to escalating petroleum product prices. It is the main challenge of the twenty-first century. To overcome those things, we are in a position to make the best replacement for fossil fuels that can be generated from existing national resources.[1] Biodiesel production from jatropha curcas, Calophyllum inophyllum, and Ceiba pentandra through a two-step transesterification process. The methanol and oil ratio of 9:1 with preheat temperature at 60°C for 60 min in the presence of 1% KOH yields lower acid values and high methyl ester.[2] The optimal working level for the B50 punnai oil blend operated diesel engine was 80°C intake air temperature, 250 bar injection pressure, 18.5 Compression Ratio (CR) and 25°C TDC injection time.[3] The performance test conducted in an engine fuelled with a rapeseed methyl ester. B5 and B20 blend of biodiesel reduce carbon monoxide (CO) emissions by 9% and 32%, respectively. From the combustion analysis, there is a shorter ignition delay for rapeseed biodiesel as compared to neat diesel fuel.[4]

The research work carried out in the diesel engine operated with palm biodiesel. The fuel properties are most suitable for an engine operation. Palm biodiesel minimizes the engine emission parameters like CO, hydrocarbon (HC), smoke, and PM except for oxides of nitrogen (NO_x).[(Ref.5)] The experimental work conducted on a Compression Ignition (CI) engine fuelled with Palm, Mustard, and Calophyllum biodiesel samples. The B20 biodiesel blend showed better performance as compared to other biodiesel blends. The Brake specific fuel consumption (BSFC) and BP of the B20 blend are improved by 12% and 7.7%, respectively, as compared to other blends also the CO and HC were reduced by 43% & 68%, respectively.[6] The essential properties of Calophyllum inophyllum biodiesel are similar to diesel fuel for use in CI engines.[7] It is evident from the literature, that the various biodiesels have been used to test the characteristics of the CI Engine. The Brake thermal efficiency (BTE) for all biodiesel blends has decreased and the optimal blend ratio (biodiesel & diesel) is about 20:80. Furthermore, the NO_x emission increased for all biodiesel blends. The engine emissions of HC, CO, and smoke reduced substantially under all conditions. The major biodiesels used in the CI engine are Annona oil, Jatropha oil, Karanja, Punnai, Pongamia pinnata, etc.[8]

The concept of a thermally coated engine is to reduce the loss of heat from the Ccombustion Chamber (CC) of the engine to the engine coolant. The diesel

engine was investigated with B25 rubber seed biodiesel. The combustion chamber parts are coated with alumina ceramic material. The BTE was increased by 4% and BSFC decreased by 9% for B25 biodiesel operated in the coated engine. The peak Cylinder Pressure (CP) and Heat Release Rate (HRR) increased when the engine's operated in coated condition.[9]

An investigation carried out in a Thermal Barrier Coated (TBC) CI engine operated with diesel as fuel. The ceramic coating materials (88% YSZ, 4% MgO, and 8% TiO_2) were coated over the combustion chamber parts 150 μm thick by plasma spray technique. The BTE increased by 10% and BSFC decreased by 9.8%. The engine exhaust emission parameters are decreased except NO_x.[(Ref.10)] The performance of TBC diesel engines was analyzed with the upper surface of the combustion chamber parts coated with three different ceramic materials. The bond coat of NiCrAl used to deposit on the combustion chamber parts. The BTE increased by 12.1% and BSFC decreased by 16.2%. The coated engine HC, CO & smoke emissions decreased by 17.8%, 18.4%, and 14.87%.[11]

An experimental work conducted on DI water-cooled diesel engine fuelled with B25 Moringa oleifera biodiesel blended with conventional diesel. The combustion chamber was coated with an YSZ TBC material. Pyrogallol additive with a quantity of 1% was added to the biodiesel for improving the physical and chemical properties. The CE operated with prepared biodiesel and additive blend showed better BSFC & BTE when compared to the UCE. The emission of CO, HC, and CO_2 was reduced considerably with a blend of biodiesel and additive.[12] The outcome of ZrO_2 coating on engine performance operated with cottonseed oil and sunflower oil methyl ester (CME & SME) carried out on diesel engine. There is an improvement in BP, MEP, and BSFC when the engine is operated with CME and SME in CE because of the reduced heat penetration through the wall. The reduced emissions were recorded owing to the surplus oxygen in the vegetable oil helps to enhance the combustion rate.[13]

The research work carried out on the TBC diesel engine operated with ultra-low sulfur diesel blended with 20% waste frying cottonseed oil. The combustion chamber coated with the TBC of zirconium oxide with 400-micron thickness. The results showed that the BTE of the coated engine (CE) increased and engine emission decreased while compared to the uncoated combustion engine (UCE). The HRR occurred earlier in the CE to the UCE with increased NO_x emission. Finally, it has been noted that numerous investigations were conducted in a diesel engine using various coating materials such as partially stabilized zirconia, titanium, alumina, mullite, yttria-stabilized zirconia, magnesium oxide as the TBC material. The TBC in the engine improves the engine performance such as BTE and SFC but due to the rich combustion chamber temperature, the NO_x emission increased. Many researchers have recorded that the combustion characteristics have improved with the usage of TBC engines with biodiesels.[14]

Usage of nanoparticles as gasoline additives improves the properties such as mass diffusivity, thermal conductivity, and high surface-area-to-volume ratio. Nanoparticles, blended in a small proportion with biodiesel and diesel, have the potential to reduce NO_x emissions. CuO nanoparticles were added to the 20% Mahua biodiesel blend (MME20) with 50 ppm and 100 ppm using an ultrasonicator. They noticed that there was a significant enhancement in the engine performance.[15] Effect of the addition of cerium oxide (CeO_2) nanoparticles in castor oil biodiesel on the IC engine examined. During this study, the BSFC and BTE improved and ignition delay decreased with the addition of CeO_2 and ethanol in diesel fuel. The CeO_2 nanoparticles enhance the complete combustion.[16]

Effect of nanoparticles with Pongamia methyl ester (PME) on the diesel engine was investigated. In this study ferro fluid, nanoparticles were prepared and mixed with biodiesel blend at 1%, 2%, and 3% as volumetric based nanoparticles with water as the base and citric acid as the surfactant. The result seen that BSFC was reduced by 8% compared to PME biodiesel. The emission characteristics were also reduced when the engine operated with ferrofluid blended PME biodiesel.[17] The impact of CuO nanoadditive with Momordica Charantia biodiesel (MCME) in a CI engine was examined. The MCME blended with neat diesel to prepare blends of 10%, 20%, 30%, and 40%. The blends are mixed with the CuO nanoparticles with a 1% volumetric proportion. The experiment outcomes showed that the B20 fuel (79% diesel + 20% MCME + 1% CuO) gives better performance than other biodiesel blends.[18]

The outcome of CeO_2 nanoadditive blended with palm biodiesel coated engine investigated. The partially stabilized zirconia (PSZ) and aluminium

oxide (Al_2O_3) ceramic powder are used to coat the engine combustion parts using the plasma spray technique. The final result showed an increment in BTE of 3.21%, 4.28%, and 4.82%, and a decrement in SFC of 11.86%, 16.92%, and 20.57% when the engine is operated with neat palm biodiesel and added CeO_2 to the biodiesel with the proportion of 30 ppm and 60ppm. Additionally, the use of the CeO_2 nanoparticles in biodiesel has reduced the NO_x emission by 2.4%.[19] Effect of Al_2O_3 nanoadditive blended with the Pongamia Methyl Ester (PME) were studied. The B20 PME was mixed with the Al_2O_3 nanoparticles in the quantity of 25, 50, and 100 ppm. The study found that the addition of Al_2O_3 with PME fuel gave better performance results as compared to diesel. Finally, the study concluded that the mixing of 50 ppm Al_2O_3 with PME biodiesel produces better results in diesel engines as compared to PME biodiesel and diesel.[20] The impact of silver nanoparticles blended with Honge Oil Methyl Ester (HOME) in a DI diesel engine examined. The silver (Ag) nanoparticles blended with HOME biodiesel in a mass fraction of 25 ppm and 50 ppm. The test results showed that the HOME + 50Ag fuel gives better results than the HOME + 25Ag and neat diesel.[21] From an aforesaid literature review, it has been noted that numerous investigations were performed in a diesel engine using various nanoparticles as additives mixed with biodiesel such as CeO_2, TiO_2, Al_2O_3, MgO, SiO_2, ZnO, and CuO. When nanoadditives have blended with biodiesel, they have shown a better reduction of the NO_x emission.

Most of the researchers are suggested that Yttria Stabilized Zirconia (YSZ) is a prominent TBC material used in engines. For improving the corrosion opposition, TBC was selected in the present study with a combination of 88% YSZ, 8% TiO_2 and 4% MgO was used as the coating material. TiO_2 and MgO ceramic material phases serve as sealing holes, releasing tension and decreasing cracks on the sections of the combustion chamber.[22]

From the literature review, it is found that the effect of a mixture of thermal barrier coating (YSZ-MgO-TiO_2) provided on the engine components with the minimum thickness (less than 200 μm) was not extensively studied in the diesel engines. The quantum of work carried out with the combination of coating on the combustion chamber parts with YSZ-MgO-TiO_2 fuelled by punnai methyl ester with the addition of CuO nanoadditives on water-cooled DI diesel engines with combustion studies is limited. The simultaneous reduction of NO_x and smoke emission along with increased thermal efficiency using nanoadditive in biodiesel identified in this work.

Experimental Section

Test fuel

A Punnai kernel was acquired from a forest area near Sathyamangalam, Erode District, India. The photographic image of punnai fruit, dried punnai kernels, and punnai oil is shown in Fig. 1. The prepared oil is converted into punnai biodiesel by a two-step transesterification process. Fig. 2 shows the layout of making punnai biodiesel from punnai oil. The prepared PME was mixed in two different preparations with diesel: PMEB20 (20% PME with 80% neat diesel) and PMEB20 + CuO 50 (prepared PMEB20 with 50ppm CuO nanoadditive). The photographic view of CuO powder, probe sonicator, and mixing of 50ppm CuO nanoadditive with PMEB20 is shown in Figs 3 (a) (b) & (c), respectively. The 10 ml of SDS surfactant dispersed with the prepared copper oxide nanoadditive. The fuel properties and the details of CuO nanoadditive were shown in Table 1 & 2.

Thermal barrier coating

Initially, the engine parts were coated with NiCrAl by plasma spray technique, and after that were coated with a mixture of 150 μm thick consisting of 88% YSZ, 8% TiO_2 and 4% MgO. Fig. 4 shows the TBC-coated parts of the engine. Tables 3 and 4 show the specifications for plasma spray coating and TBC materials.

Size of the nanoadditives

The size of nanoadditive particles plays an important role in yielding expected enhancement. Hence, it is decided to employ that the diameter of the nanoparticles should be less than 100 nm. For the measurement of the size of the particles, HR-SEM analysis was carried out and shown in Fig. 5. From the images, it is ensured that all the particles are of diameter less than 100 nm. The HR-SEM image exposed that the CuO prepared with the particle size of 23 nm has a sphere-like structure. The technical features of the test engine are listed in Table 5. The photographic view and schematic view of the test setup are displayed in Figs 6 and 7, respectively. The accuracy of the test instruments was displayed in Table 6. The required amount of the nanoadditive samples is weighed accurately using electronic

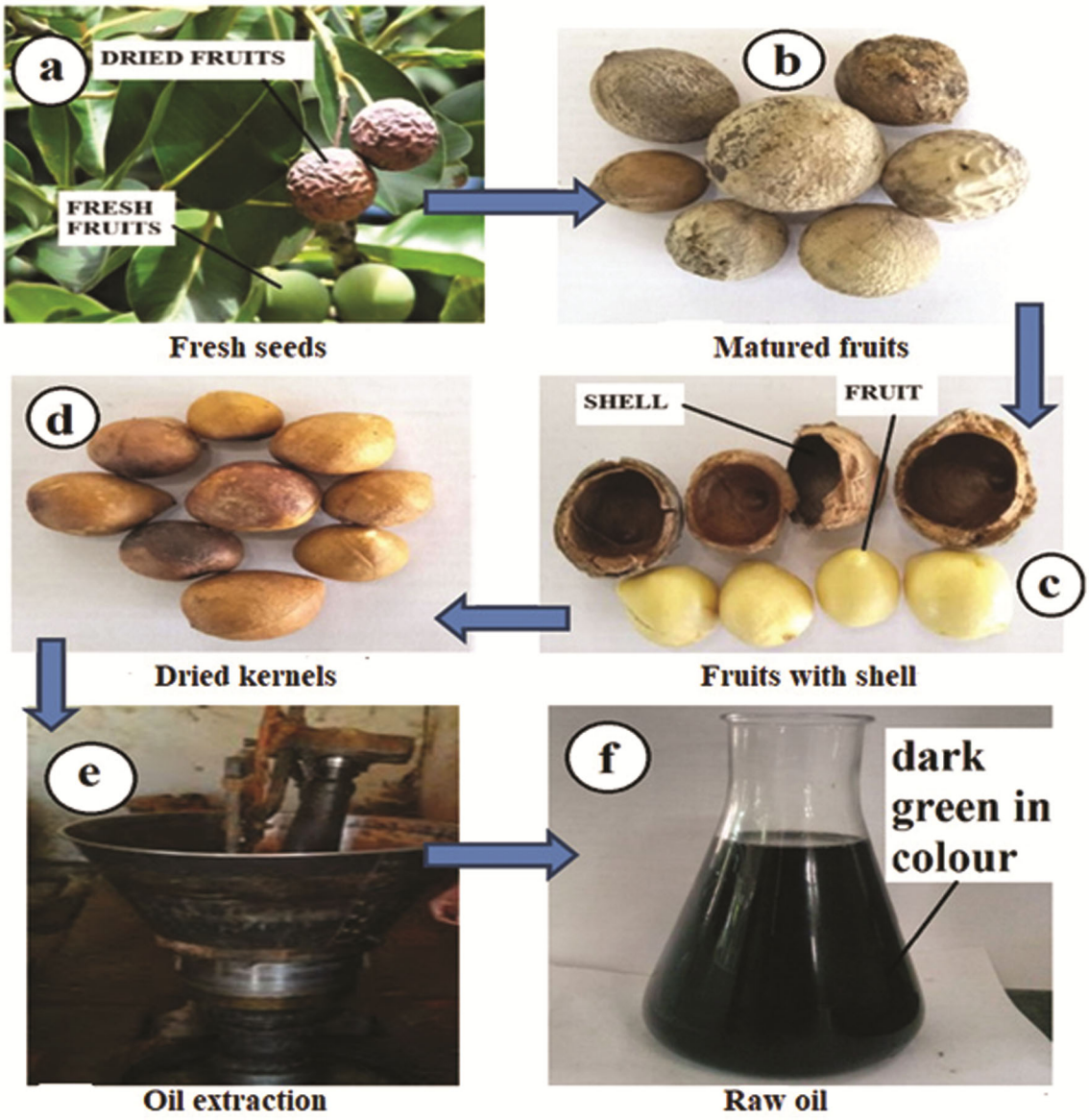

Fig. 1 — Extraction of Punnai oil from matured fruit

analytical balance for every dosing level and dispersed thoroughly in the fuel, using an ultrasonic shaker, giving a constant agitation time of 30 min to ensure uniform suspension and stable nanofluid. The Sonication bath improves the dispersion phenomenon of nanoadditive with PMEB20. During the initial testing stages of nanoadditives, they are found to dissolve in water and also in other chemical solvents. The direct mixing of nanoadditives in PMEB20 results in complete settling down of nanoadditives. Ultrasonication bath enhances the dispersion property of nanoadditives in prepared biodiesel blend using sonicator there by controlling the particle sedimentation. The modified fuel is then subjected to experiments immediately after the preparation to bring out the improved properties of PMEB20 fuel.

Results and Discussion

The experiments were conducted for diesel, PMEB20, and PMEB20 + CuO 50 fuel samples in uncoated and coated engines. The FTIR and GD-MS analysis of the prepared punnai biodiesel are carried out and discussed. In this experimental investigation, the repeatability of the experiments initially taken as three to four times for all the engine output characteristics operating with both diesel and biodiesel fuel also this repeatability of the experiments would be included in the experiment uncertainty analysis.

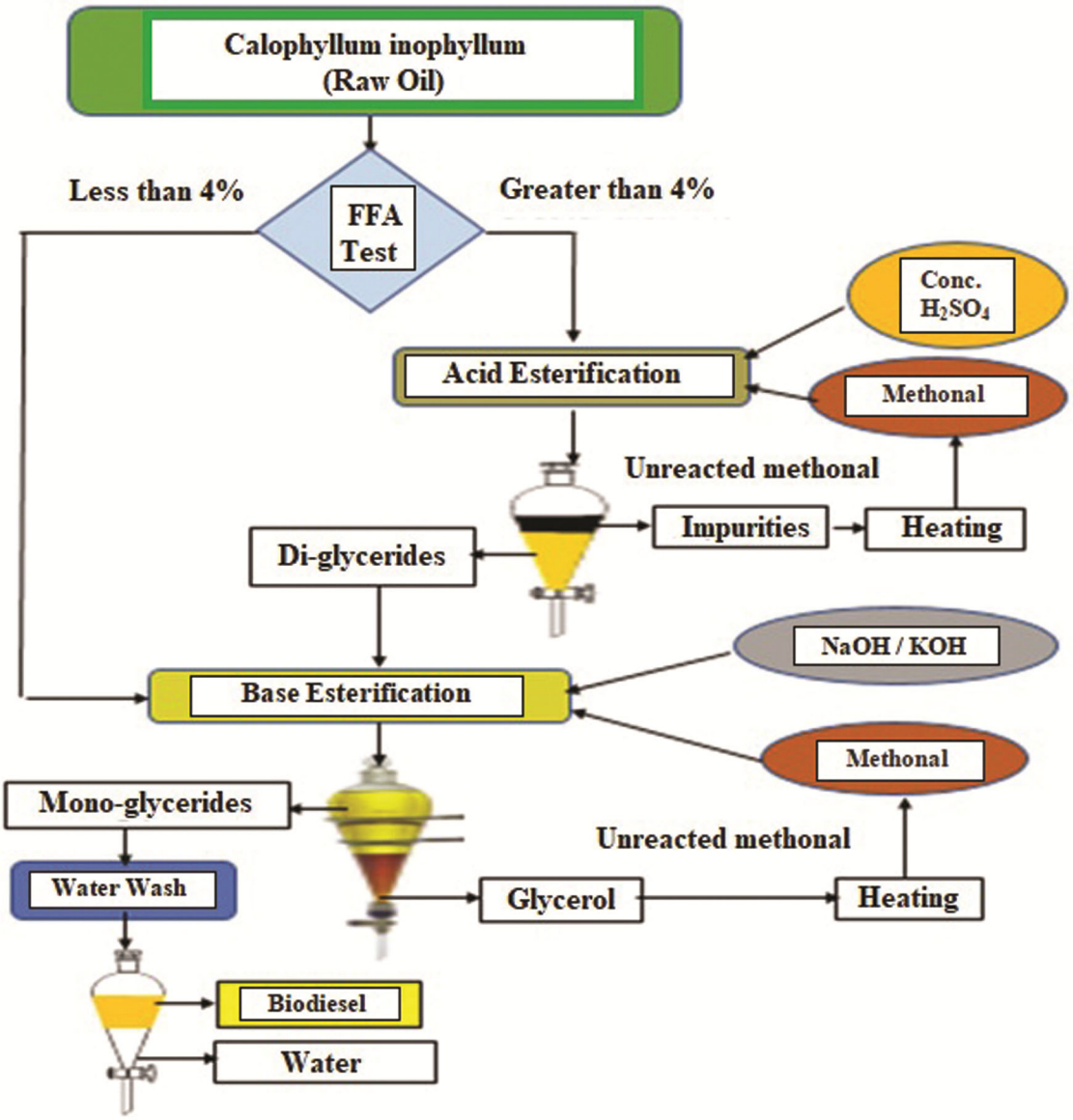

Fig. 2 — Layout of Punnai seed oil methyl ester production

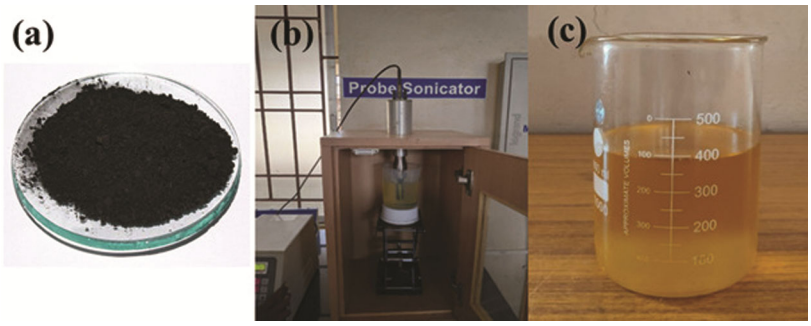

Fig. 3 — (a) CuO nanoadditive (b) Probe sonicator and (c) B20 Punnai Methyl Ester mixed with 50ppm CuO nanoadditive

Table 1 — Properties of the test fuels

Property	Testing methods	Diesel	PMEB20	PMEB20 + CuO 50
Density (kg/m^3)	ASTM D127	830	867	855
Kinematic Viscosity at 40°C (m^2/s)	ASTM D445	3.07	5.88	4.88
Gross Calorific Value (kJ/kg)	ASTM D240	44125	39020	40120
Flash Point (°C)	ASTM D93	56	76	72
Fire Point (°C)	ASTM D93	64	89	78

Table 2 — Properties of Copper oxide

Item	Specification
Molecular formula	CuO
Molecular weight	79.5 g/mol
Appearance (color)	Black
Appearance form	Powder
Size	40 nm

Table 3 — Details of plasma spray coating

Nozzle	GH Type
Argon gas pressure	100–120PSI
Hydrogen gas pressure	50PSI
Distance of spraying	7.6 m – 12.7 m
Current (A)	490-500
Voltage (V)	60-70
Particle velocity	Up to 450 m/s
Arc temperature	16000°C

Table 4 — Properties of TBC materials

Materials	Thermal Conductivity (W/mK)	Thermal Expansion 10^{-6} (1/K)	Melting Point (°C)
YSZ	1	10.9	2980
MgO(4%)	30	12	3135
TIO_2 (8%)	3.3	9.4	2123
NiCrAl (bond coat)	15	19	1673

Table 5 — Details of the test engine

Type	4 stroke, direct injection, diesel engine
Rated power	5.2 kW at 1500 rpm
Injection pressure	210 bar
Dynamometer	Eddy current

Table 6 — Accuracy of the instruments

Instruments	Accuracy
Gas analyzer	±0.02% CO, ±0.03% CO_2, ±20 ppm HC and ±10 ppm NO_x
Smoke	±0.1%
Temperature indicator	±1 °C
Speed	±10 rpm
Load	±0.1 kg
Burette for fuel measurement	±0.1 cc
Digital stopwatch	±0.6 sec
Manometer	±1mm
Crank angle encoder	±10

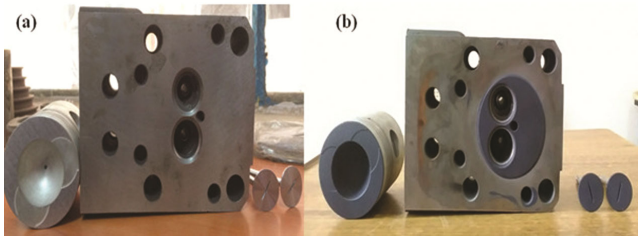

Fig. 4 — TBC parts of the engine

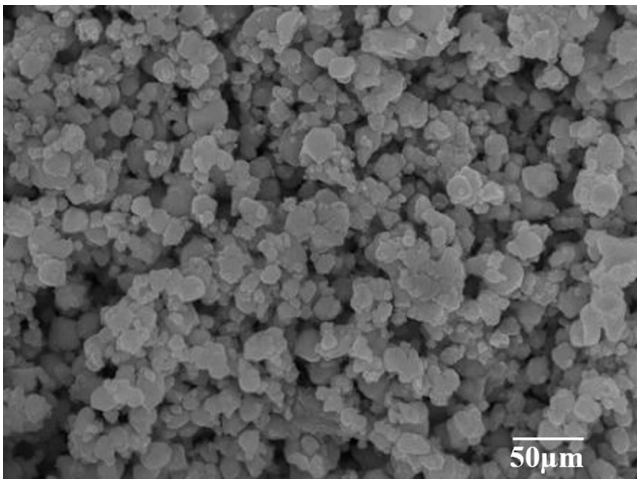

Fig. 5 — HR-SEM image of CuO nanoadditives

Fig. 6 — Pictorial view of the test setup

FTIR Analysis

It is identifying the frequency range where infra-red absorption occurs for the prepared biodiesel. Punnai oil methyl ester was studied for its functional groups, chemical bonds, and vibration type. Fig. 8 shows the FTIR spectrum of the punnai oil methyl ester. Table 7 depicts the intensities of distinct bond types found in biodiesel. The FTIR spectrum

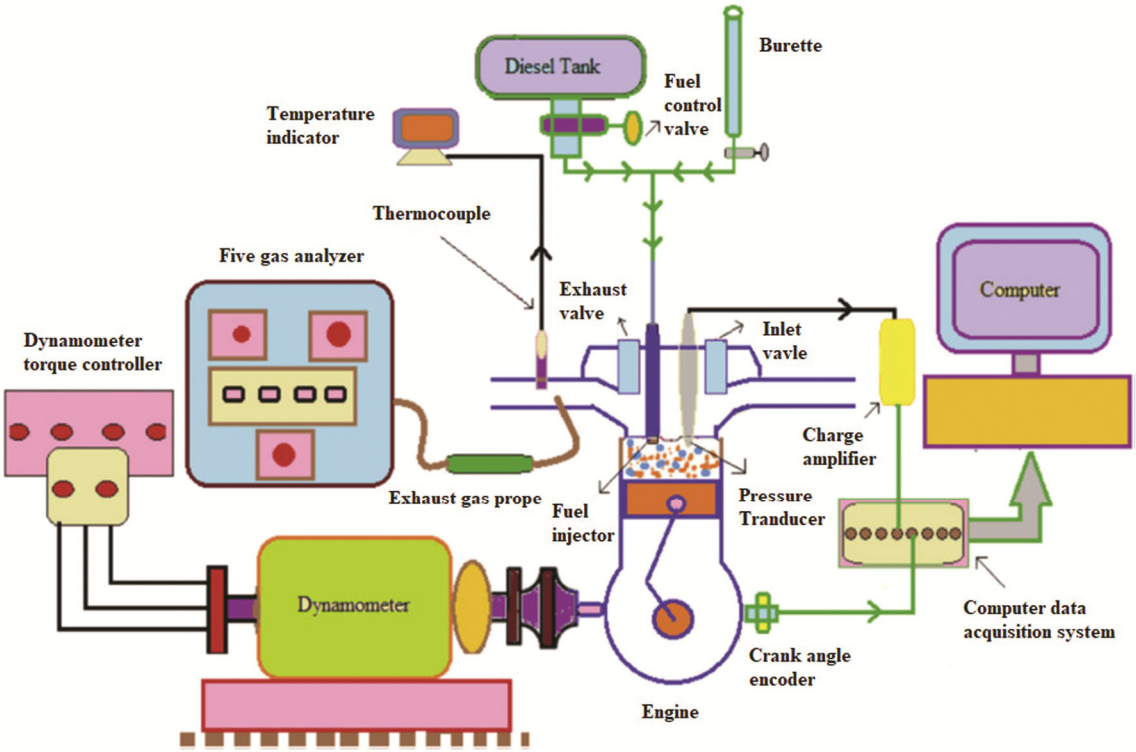

Fig. 7 — Schematic of the test setup

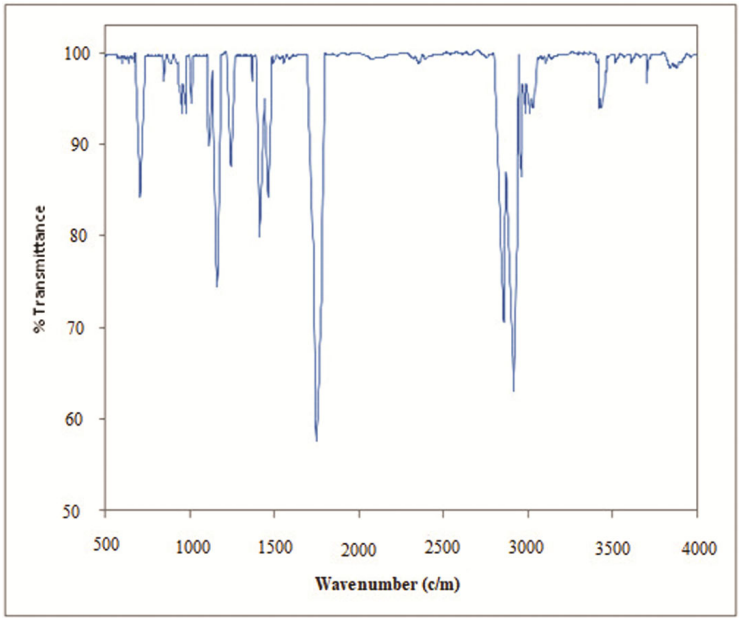

Fig. 8 — FTIR spectra of Punnai Methyl Ester

of PME showed the bands at 3434.3 cm^{-1} and 3023.59 cm^{-1} indicating the presence of amides and alkenes with C=O, N-H, =C-H, and C=C bonds. The band at 2915.61 cm^{-1} exhibited a C-H bond type alkane, functional group. The stretch at 1748.91 cm^{-1}exhibited N-H bond type ketones in the biodiesel. The C=C stretch at 1463.59 cm^{-1} and N-O bond at 1369.10 cm^{-1}indicates the presence of aromatics and nitro components in the biodiesel. The C-H and –C-H vibration at 1243.76 cm^{-1} indicates the

presence of alkenes. The absorption peaks at1160.84cm^{-1} and 1114.56 cm^{-1} revealed the presence of amines and alcohols in PME. The crest at bands 1010.43 cm^{-1} represented the presence of an alcohol group with a C-O bond. The =C-H band at 956.44 and 846.5.36 cm^{-1} indicated the presence of alkene as a functional group in PME. The peak at 707.69 cm^{-1} indicates the =C-H, C=C stretching vibrations with association to the occurrence of alkene. The oxygen molecules lead to the formation of hydro peroxide, which would increase the chain reactions and accelerate the oxidation.[23]

Table 7 — FTIR analysis for Punnai biodiesel

Wavenumber (cm^{-1}) Stretch	Bond Type	Functional group	Intensity
3434.30	C = O, N-H	Amides	strong
3023.59	=C-H, =C-H, C = C	Alkene	medium
2915.61	C-H, -C-H	Alkane	strong
1748.91	N-H	Ketones	medium
1463.59	C=C	Aromatics	Weak
1369.10	N-O	Nitro	Strong
1243.76	C-H, -C-H	Alkane	variable
1160.84	C-N	Amines	Strong
1010.43	C-O	Alcohol	medium
956.44	=C-H	Alkene	variable
846.5	=C-H	Alkene	medium
707.69	=C-H, C = C	Alkene	strong

GC-MS Analysis

It is provide the details of fatty acids in the fuel. It is also used to find out the number of components in a mixture. For each identified component, the GC-MS results indicate the molecular weight and its formula, and area. The full Scan mode analysis method was applied for GC-MS. This approach detects substances within a certain range over a set length of time. The peaks were compared to the tallest peak in terms of intensity. Fig. 9 shows the GC-MS spectrum of the PME. The GC-MS peaks revealed the presence of fatty acid and esters. The major component was linoleic acid with 34.42%. The percentage of the second major component of oleic acid is 22.02%. Stearic acid and palmitic methyl acids are the third and fourth most components at 15.75% and 28.81%, respectively. The presence of fatty acids in the derived biodiesels such as palmitic acid, stearic acid, oleic acid, linoleic acid, octadecadienoic acid, octadecenoic acid, and others, makes it a viable renewable energy source for biodiesel.[23]

Performance characteristics

The BSFC for the prepared fuel samples with load in the UCE and CE is shown in Fig. 10. The quantity of fuel essential to generate a unit power output in an

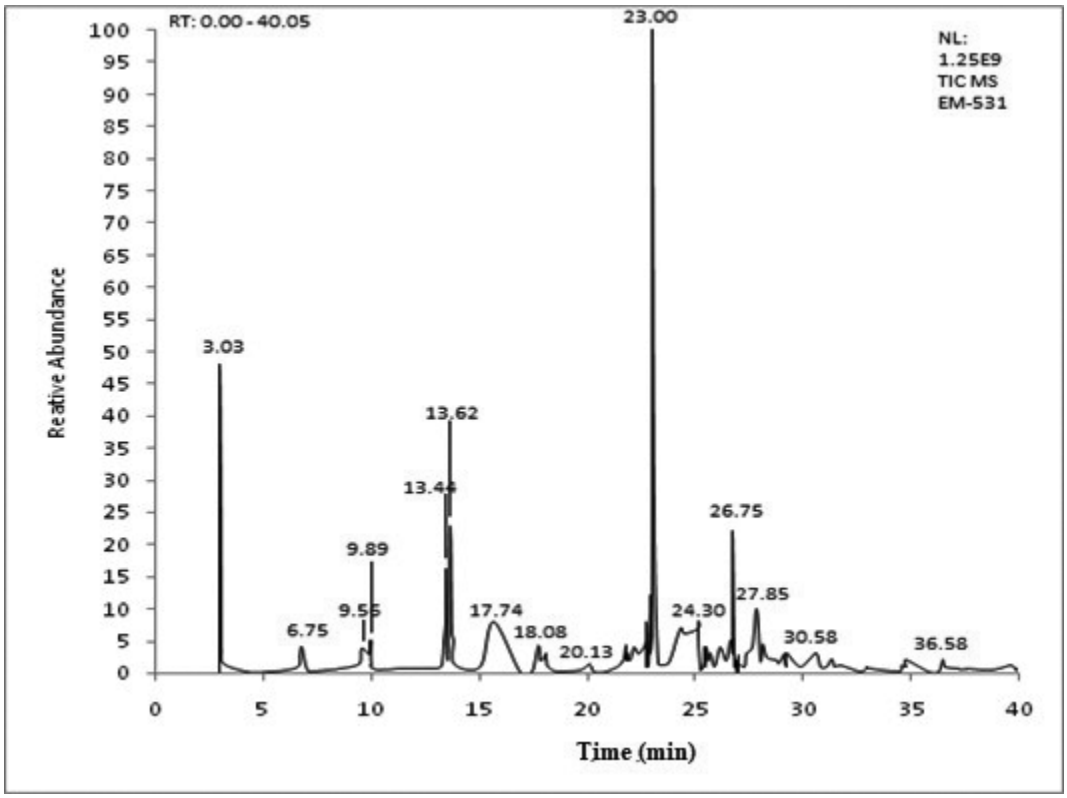

Fig. 9 — GC-MS chromatogram of Punnai Methyl Ester

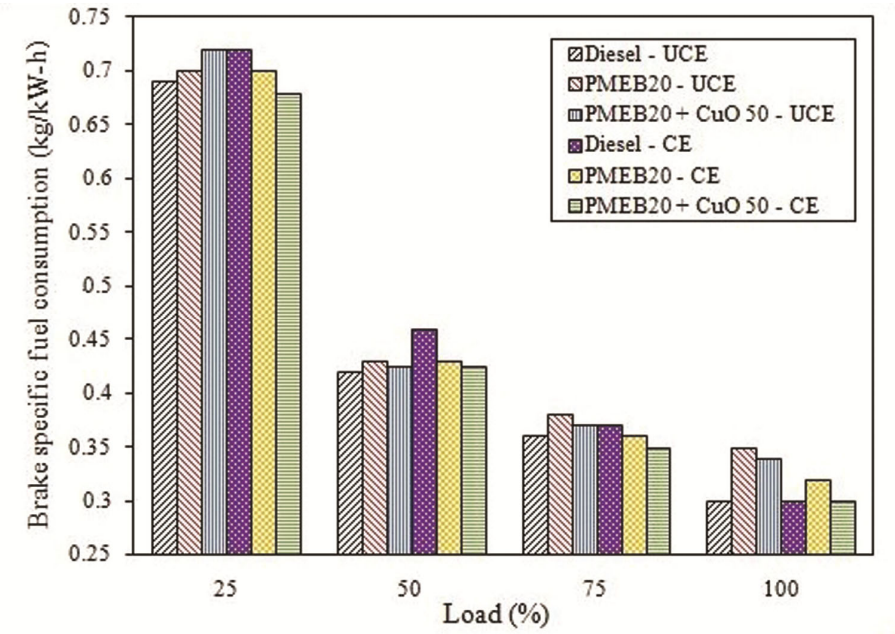

Fig. 10 — Plot of BSFC vs. load

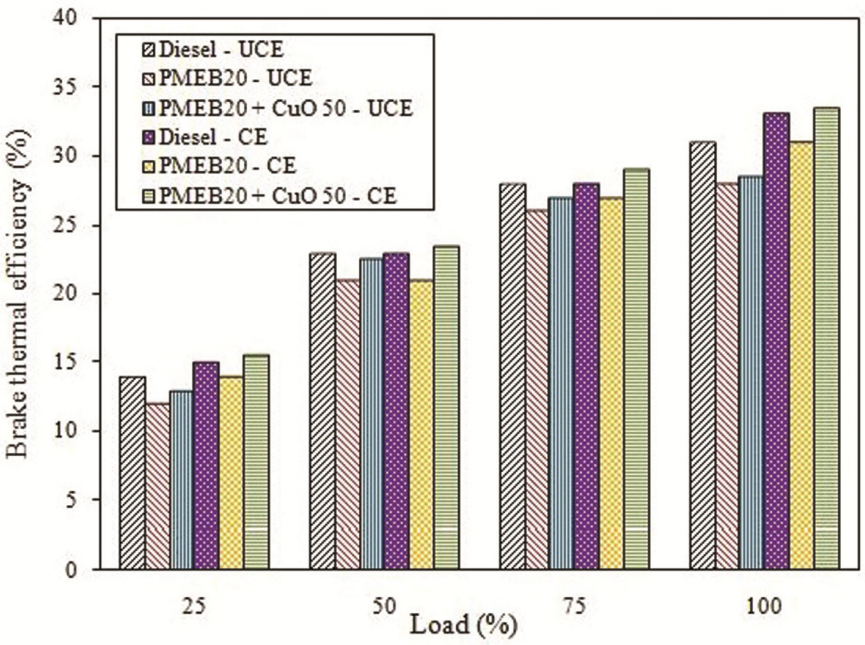

Fig. 11 — Plot of BTE vs. load

engine is known as the BSFC. The BSFC for diesel fuel, PMEB20, and PMEB20 + CuO 50 at peak load condition was 0.33, 0.35, 0.34 and 0.305, 0.32, 0.29 kg/kW-h for UCE and CE, respectively. In CE, PMEB20 + CuO 50 fuel demonstrated lowered BSFC due to the high combustion temperature and minimized heat loss from the engine. CuO enhances the combustion process and reduces fuel consumption since nanoadditives are oxidation agents that reduce CO accumulation, resulting in improved combustion.[24] The similar outcomes found using Mahua biodiesel and an aluminium silicon carbide TBC engine with a BSFC of 3.53%, which was lower than the UCE.[26]

Fig. 11 displays the difference in BTE for the prepared fuel samples with load in the UCE and CE.

The BTE, also known as gasoline energy conversion, is a measure of how much useable energy is derived from fuel. The BTE for diesel fuel, PMEB20, and PMEB20 + CuO 50 at top load applied to the engine was observed as 31%, 28%, 29.5% and 33%, 31%, 33.5% for UCE and CE, respectively. For UCE's, diesel showed peak one as compared to fuel samples due to its superior fuel properties. In CE, PMEB20 + CuO 50 fuel demonstrated peak BTE as compared to the other fuel samples. The high in-chamber temperature due to the TBC used in the combustion chamber was the main factor for the increase in BTE.[13,25] Further, the addition of CuO with PMEB20 enhanced the BTE due to the micro-explosion and secondary atomization of the nanoparticles.[17]

The EGT for the prepared sample of fuels in the UCE and CE is shown in Fig. 12. EGT is a measurement of a fuel's heating potential. Exhaust gas removes 1/3rd of heat generated by the engine. The EGT for diesel fuel, PMEB20, and PMEB20 + CuO 50 at peak load conditions were noted as 215, 220, 229 and 200, 220, 250°C for UCE and CE respectively. Due to the impact of TBC provided to the CC, the EGT value for CE's is higher than the UCE for all prepared fuel samples. Furthermore, the EGT value for PMEB20 + CuO 50 is higher due to active combustion occurring with the excessive O_2 of fuel in the nanoadditive presence and TBC applied to the engine. When nanoparticles are added to gasoline, the ignition delay (ID) is reduced while the cetane number (CN) of the fuel improves, resulting in a substantial portion of the combustion completing before TDC, resulting in enhanced combustion.[17]

Emission characteristics

Fig. 13 displays the difference in CO emission for the prepared fuel samples with load in the UCE and CE. The burning rate of the fuel-air mixture determines CO emissions, which are mostly formed by incomplete burning and insufficient oxygen. The CO emission for diesel fuel, PMEB20, and PMEB20 + CuO 50 at peak load conditions was noted as 0.080, 0.05, 0.031% and 0.073, 0.05, 0.023% for UCE and CE, respectively. The PMEB20 + CuO 50 showed lower CO emissions than the other fuel samples in both CE & UCE. This was attributed to the TBC engine's combustion chamber being sustained at a high temperature, causing less incomplete burning and the enrichment qualities of CuO nanoadditive boosting the oxidation reaction in the combustion chamber. The same result achieved with aluminium oxide and cerium oxide nanoparticles added to palm methyl ester on a yttria-stabilized zirconia coated engine.[19]

The difference in HC for the prepared fuel samples with load in the UCE and CE is shown in Fig. 14. Incomplete combustion of fuel causes HC emissions, which are caused by fuel droplets escaping into the

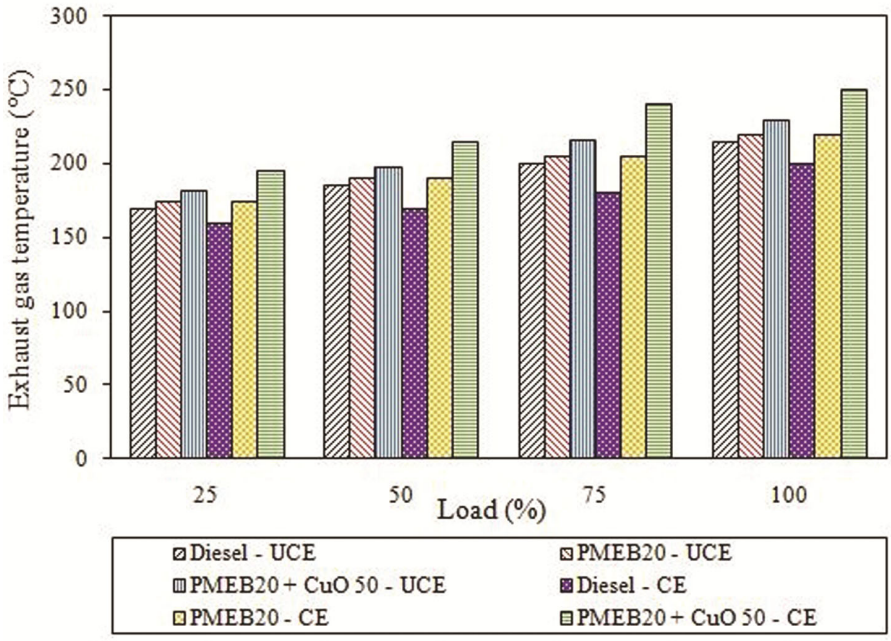

Fig. 12 — Plot of EGT vs. load

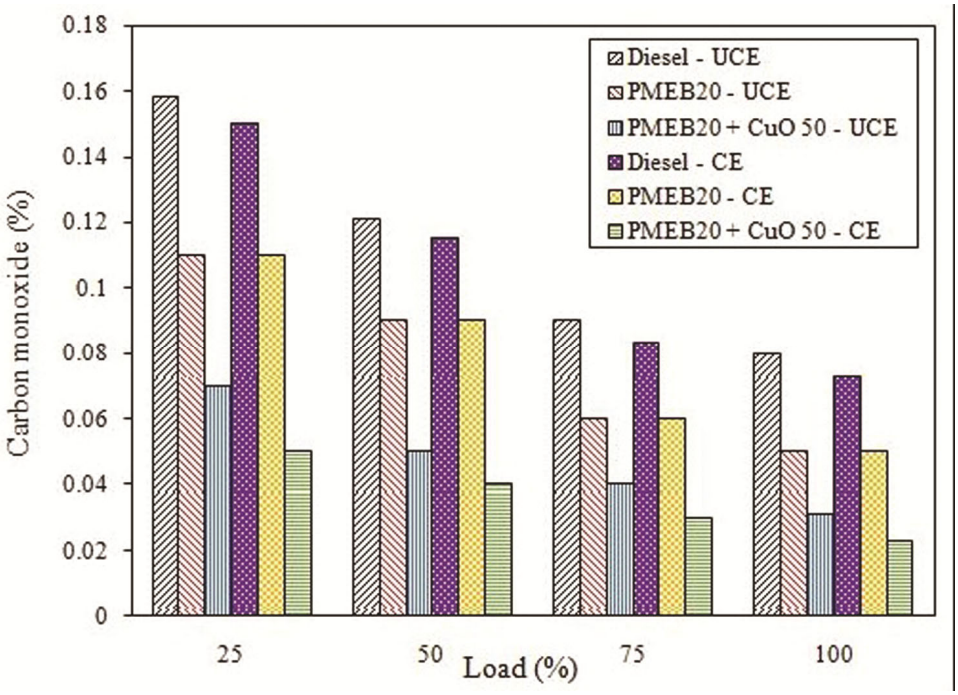

Fig. 13 — Plot of CO vs. load

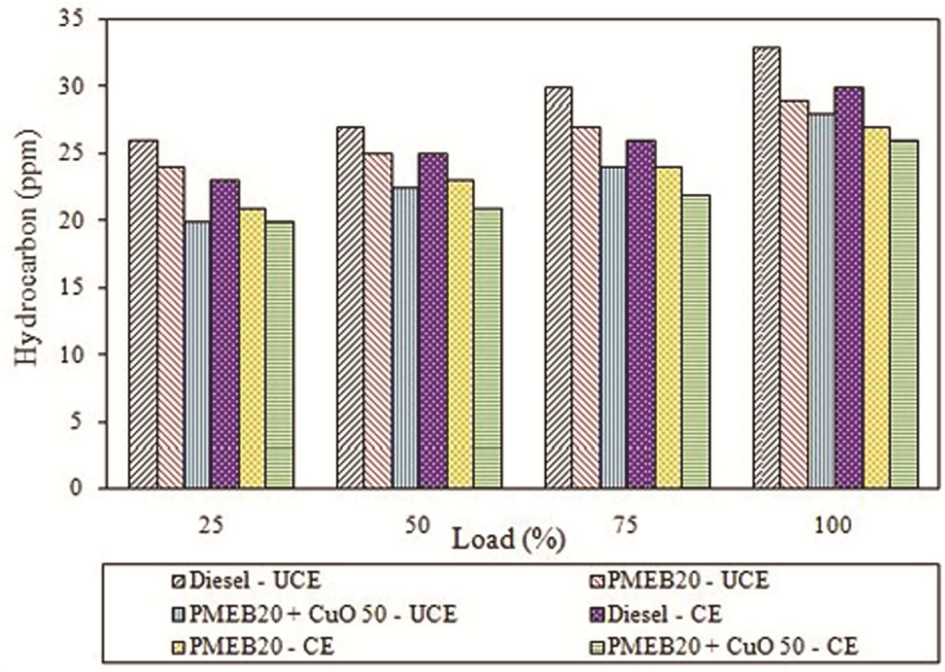

Fig. 14 — Plot of HC vs. load

gap region of the cylinder wall.[27] The HC emission for diesel fuel, PMEB20, and PMEB20 + CuO 50 at peak load conditions was detected as 33, 29, 28 ppm, and 30, 27, 26 ppm for UCE and CE respectively. In terms of CE, PMEB20 + CuO 50 showed less HC than the other fuel samples. This is due to the TBC engine's greater oxygen level and temperature, which promotes better combustion. Further, CuO has higher catalytic activity owing to its large surface area per unit volume, resulting in improved combustion. The low reaction temperature of carbon burning, the CuO oxidation agent produces complete burning of fuel by

enhancing the oxidation of hydrocarbons.[17] According to the findings, the increased lean combustibility limit and quenching range justified the reduction of HC emissions on a TBC coated engines.[28]

Fig. 15 shows the difference in oxides of nitrogen for the prepared fuel samples in the UCE and CE. The formation of NO_x is mostly caused by a rise in in-cylinder temperature. Flame combustion temperature, fuel oxygen content, and reaction time all influence NO_x generation. The NO_x emission for diesel fuel, PMEB20, and PMEB20 + CuO 50 at peak load conditions was detected as 580, 625, 528 ppm, and 595, 695, 550 ppm for UCE and CE respectively. In general, TBC engines emit more NO_x than UCE while running on biodiesel. This is owing to the biodiesel's higher oxygen concentration, shorter ID, and higher engine cylinder temperature.[14] However, when CuO was added to PMEB20 biodiesel and run in a TBC engine, the NOx emissions were displayed lower than the diesel fuel used.

The difference in smoke for the prepared fuel samples in the UCE and CE is shown in Fig. 16. The smoke level for diesel fuel, PMEB20, and PMEB20 + CuO 50 at peak load conditions was detected as 70, 68, 48 HSU, and 68, 63, 46 HSU for UCE and CE, respectively.PMEB20 + CuO 50 fuel caused lesser smoke emissions than the other fuel samples for both UCE and CE. This is owing to the availability of sufficient oxygen in biodiesel, as well as better combustion processes and increased turbulence provided by TBC, which improves combustion and diminishes smoke opacity. It was similarly noted that the addition of CuO nanoadditive to biodiesel improves fuel combustion. The results were similar to those obtained with cashew nut biodiesel and a PSZ CE[27], Pongamia methyl ester and an Al_2O_3 CE[29], and rice bran methyl ester with fly ash CE.[30] Due to the CE approach and the availability of nanoparticles in the biodiesel, all of the above-mentioned results indicated a reduction in smoke emission for an engine with biodiesel.

Combustion characteristics

Fig. 17 displays the variations of cylinder pressure for the prepared fuel samples in the UCE and CE. The A/F ratio, turbulence intensity, swirl motion, in-cylinder temperature, and pressure all affect the burning rate of fuel. Cylinder pressure (CP) was evaluated as a significant element in finding the burning properties of fuel among the factors stated above. Due to the influence of TBC and excessive levels of oxygen available in the biodiesel with CuO nanoadditive, the peak CP for PMEB20 + CuO 50 is 68 bar is nearly similar to the result obtained from the conventional fuel. This is owing to the fact that they have a reduced ID period and fuel injection timing, as well as a reduced heat loss. The same kind of outcome

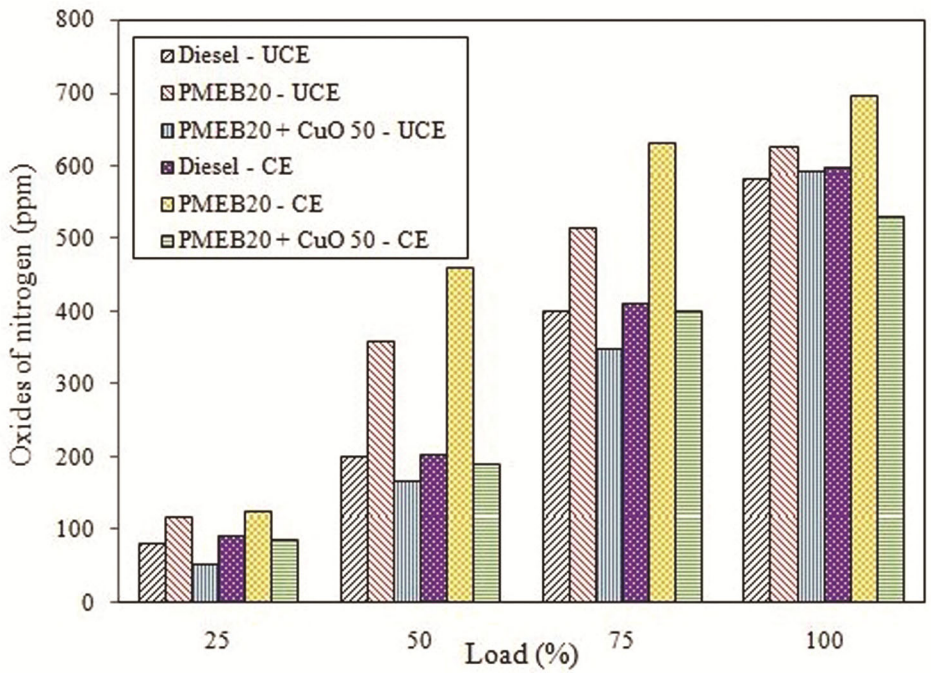

Fig. 15 — Plot of NO_x vs. load

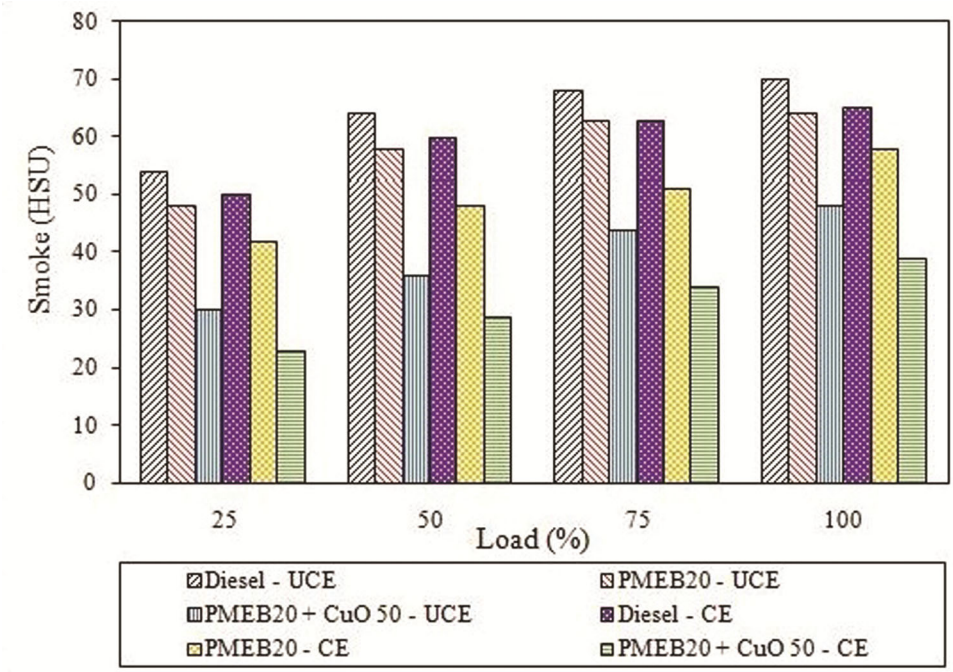

Fig. 16 — Plot of smoke vs. load

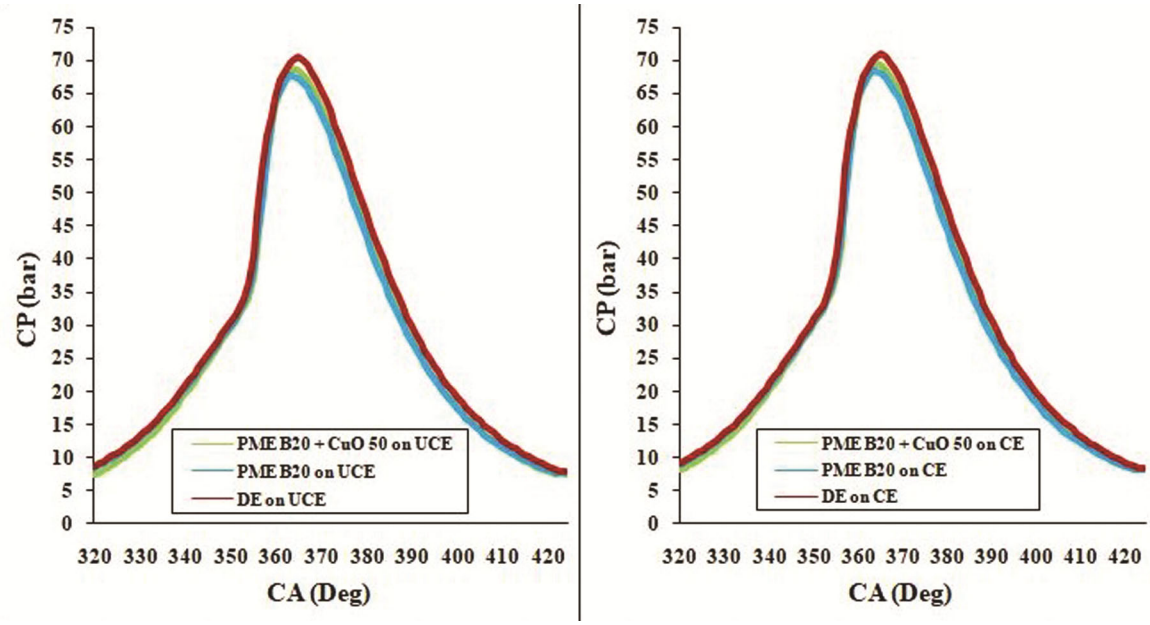

Fig. 17 — Plot of CP vs. crank angle

was founded with a B20 blend of waste cooking oil and neem biodiesel in Zirconia CE as compared with the UCE diesel as a fuel.[31, 32] The difference in HRR for the prepared fuel samples with full load conditions in the UCE and CE is shown in Fig. 18. The rate of combustion-related to the amount of chemical energy released during combustion. The figure shows that the HRR of PMEB20 + CuO 50 on CE is 63.37 J/deg, which is nearer to the 73 J/deg of diesel fuel used in a UCE owing to the shorter ID and higher CP. The higher HRR could be the outcome of the excess oxygen, the addition of nanoadditives in the fuel, and TBC provided on the engine. In a PSZ-CE, a similar kind of HRR was detected with waste frying cottonseed oil.[14]

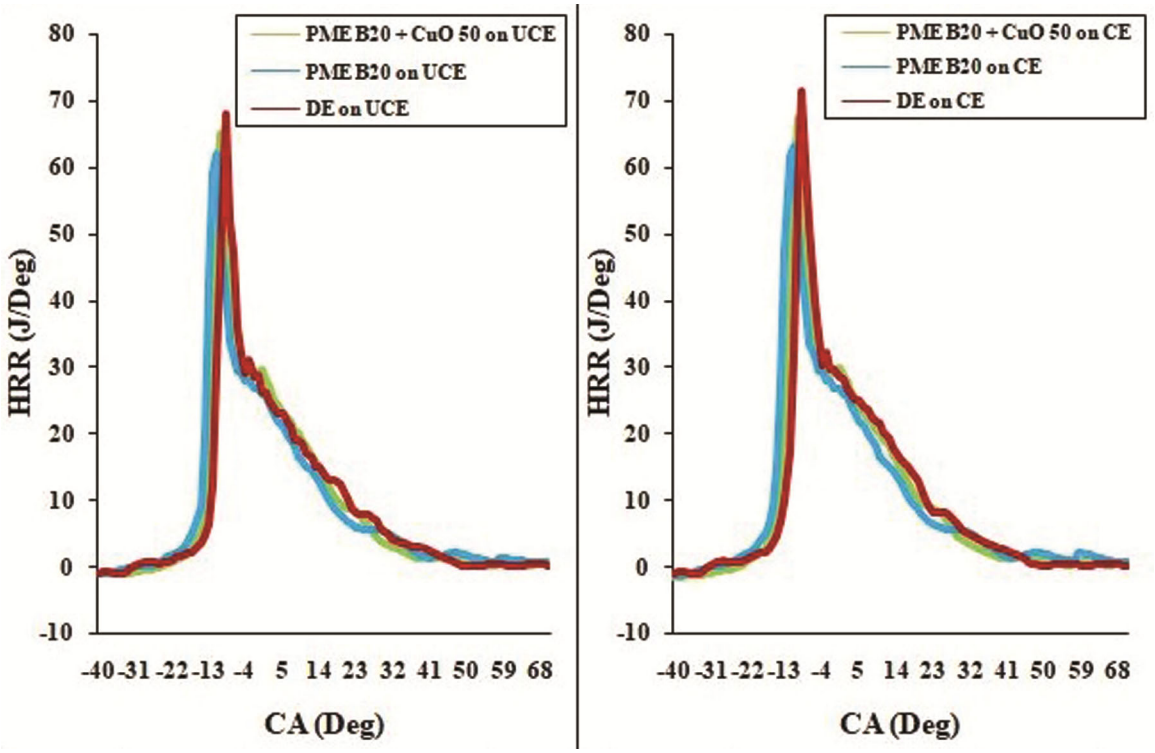

Fig. 18 — Plot of HRR vs. crank angle

Conclusion

In the investigation to study the YSZ TBC on the combustion chamber and the use of CuO nanoparticles to Punnai methyl ester in the Kirloskar TV1 model DI engine. The following is a summary of the findings:

(1) The FTIR and GC-MS analysis help to find the functional groups and fatty acid composition in the prepared methyl esters.

(2) For neat diesel fuel, PMEB20 fuel, and PMEB20 + CuO 50 the BSFC level used in CE decreased by an average of 8.09%, 9.57%, and 11.76%, respectively as compared to the UCE.

(3) For neat diesel fuel, PMEB20 fuel, and PMEB20 + CuO 50 the BTE used in CE increased by an average of 6.45%, 10.71%, and 17.54%, respectively relative to the UCE.

(4) The higher combustion output was achieved in CE owing to reduced incomplete combustion and the quantity of CO and HC were quite low.

(5) The NO_x level in the CE operated with PMEB20 was high, but it was reduced by an average of 10.84% by using 50 ppm CuO mixed with the PMEB20 fuel compared to the UCE.

(6) In comparison to the UCE, smoke emission decreased in diesel, PMEB20, and PMEB20 + CuO 50 that used CE by 7.7%, 10.34%, and 23.4%, respectively.

(7) In the CE, higher CP and HRR were observed for PMEB20 with a mixing of 50 ppm CuO nanoadditive, and it's nearer to diesel-operated in a UCE.

Hence, it can be concluded that PMEB20 with 50 ppm CuO was said to be the prominent substitute for the diesel fuel under YSZ + MgO + TiO_2 thermal barrier coated conditions. The BTE and NO_x emission for the nanoadditive disseminated biodiesel blend in the coated engine was considerably enriched compared to the normal operating condition in the engine. The major limitations of the present study are more plantation land area required for biodiesel preparation and its preparation cost was expensive. Biodiesel produce higher oxides of nitrogen (NOx) emission. Direct implementing biodiesel usage in an existing engine need very precise control and fuel metering systems.

References

1 Ramadhas A S, Jayaraj S & Muraleedharan C, *Renew Energy*, 29 (2004) 727.

2 Silitonga A, Ong H, Mahlia T, Masjuki H, Badruddin I A & Fayaz H, *Renew Sust Energy Rev*, 18 (2013) 211.

3 Narendranathan S, Sudhagar K & Karthikeyan R, *Energy Environ*, 30 (2019) 732.
4 Ekrem Buyukkaya, *Fuel*, 89 (2010) 3099.
5 Mosarof M, Kalam M, Masjuki H, Ashraful A, Rashed M, Imdadul H & Monirul I, *Energy Convers Manag*, 105 (2015) 617.
6 Sanjid A, Masjuki H H, Kalam M, Rahman S A, Abedin M & Fattah I R, *RSC Advances*, 5 (2015) 13246.
7 Sahoo P, Das L, Babu M & Naik S, *Fuel*, 86 (2007) 448.
8 Atabani A & da Silva César A, *Renew Sust Energ Rev*, 37 (2014) 644.
9 Senthil K S, Purushothaman K & Rajan K, *Therm Sci*, 221 (2017) 489.
10 Vadivel A & Periyasamy S, *J Appl Fluid Mech*, 13 (2020) 1157.
11 Reddy G V, Rasu N G & Prasad T H, *Int J Ambient Energy*, 42 (2019) 1.
12 Karthickeyan V, *Fuel*, 235 (2019) 538.
13 Aydin H, *Appl Therm Eng*, 51 (2013) 623.
14 Aydın S, Sayın C & Altun S, *Int J Green Energy*, 13 (2016) 1102.
15 Aalam C S & Saravanan C G, *Ain Shams Eng J*, 8 (2017) 689.
16 Selvan V A, Anand R B & Udayakumar M, *J Eng Appl Sci*, 4 (2009) 1819.
17 Kumar S, Dinesha P & Bran I, *Energy*, 140 (2017) 98.
18 Shaisundaram V, Chandrasekaran M, Shanmugam M, Padmanabhan S, Murali R M & Kari K L, *Int J Ambient Energy*, 42 (2019) 1.
19 Thiruselvam K & Ganesh V, *J Oil Palm Res*, 31 (2019) 138.
20 Sivakumar M, Sundaram N S & Thasthagir M H S, *Renew Energy*, 116 (2018) 518.
21 Banapurmath N, Narasimhalu T, Hunshyal A, Sankaran R, Rabinal M H, Myachit N & Kittur R, *Int J Sust Energy*, 3 (2014) 150.
22 Jia S K, Zou Y & Xu J Y, *Trans Nonferrous Met Soc China*, 25 (2015) 175.
23 Rashed M M, Kalam M A, Masjuki H H, Rashedul H K, Ashraful A M, Shancita I & Ruhul A M, *RSC Adv*, 5 (2015) 36240.
24 SoukhtSaraee H, Jafarmadar S & Taghavifar H, *Int J Environ Sci Technol*, 12 (2015) 2245.
25 Karthickeyan V, Balamurugan P & Senthil R, *J Braz Soc Mech Sci Eng*, 39 (2017) 1823.
26 Ravikumar V, Senthilkumar D & Solaimuthu C, *Int J Ambient Energy*, 34 (2013) 131.
27 Vedharaj S, Vallinayagam R & Yang W M, *Exp Therm Fluid Sci*, 53 (2014) 259.
28 Subramaniam D, Murugesan A & Avinash A, *Int J Ambient Energy*, 35 (2014) 30.
29 Mohamedmusthafa M, Sivapirakasam S P, Udayakumar M & Balasubramanian K R, *Environ Prog Sust*, 31 (2012) 676.
30 Mohamed Mu M, Sivapirakasam S P & Udayakumar M, *Energy*, 36 (2011) 2343.
31 Karthickeyan V, *Heat Mass Transf*, 54 (2018) 1961.
32 Karthickeyan V, Balamurugan P & Senthil R, *Biofuels*, 10 (2019) 207.